Seismic characterization of fractures in a naturally fractured gas reservoir

Reeshidev Bansal, Matthias G. Imhof, Seismic Reservoir Characterization Laboratory, Virginia Tech, and Thomas Daley, Lawrence Berkeley National Laboratory*

Summary

We present an approach to locate fractures in a naturally fractured Gas Reservoir using seismic reflection methods. Current commercially available technology is often able to locate the fracture zones and fracture orientation, but lack the precision and accuracy to guide a well straight into a fracture. Numerical models have shown that on seismograms, fractures are manifested in a form similar to diffraction patterns. With appropriate imaging, it may be possible to see fractures. Hence, we examine and compare various preprocessing schemes which enhance diffractions and reduce reflections in a seismogram

Introduction

Fracture patterns, which may control flow and transport properties in a naturally fractured gas reservoir play a great role in siting production wells. Hence for successful operation of the production wells, it is very important that the exact location and orientation of the fractures or the fracture swarm is known. In the past, there have been many works on characterizing the fractures especially using anisotropy in P-wave and S-wave data. S-waves while propagating through a fracture zone are polarized parallel and perpendicular to the fracture orientation and reveal different properties of the media depending upon the polarization direction (Lynn et al., 1995). Another approach is P-wave AVO analysis, which reveals the difference in poisson's ratio on different seismic lines depending on the presence of gas filled fractures. Lower poisson's ratio compared to the normal poison's ratio in the area suggests the presence of gas filled fractures (Lynn et al., 1995). These methods are capable of locating the fracture zones and fracture orientations, but they are unable to provide the exact location of fractures. The biggest constraint of these methods is that they only give good results when fractures are aligned. These methods do not include complex wave phenomena such as diffraction off fracture tips, fracture head waves and fracture channel waves. These wave phenomena are potentially more sensitive to fracture properties and geometry, and hence might reveal new information. Here we develop the processing schemes to enhance these fracture signals.

Response of the fractures in a seismic section

LBNL developed a subsurface model with five layers and two fracture sets (Daley, et al., 2002). The seismic response of this model (fig. 2) was calculated using a finite difference algorithm with 38 receivers spaced at 60m intervals. Center frequency of the source was 50 Hz. The seismogram was generated for both vertical and horizontal components of the particle velocity. Figure 2 presents the response for the vertical component of the velocity. As expected, there are five reflection hyperbolas and a number of diffraction-like signals generated by the fractures. This suggests that in a seismic survey, the fracture response may resemble to the hyperbola of a diffraction point. We need to extract these patterns to find the exact location of fractures in the subsurface.

Methodologies

We have developed and examined a number of processing schemes to enhance the diffractions and to suppress the reflections in the seismic data. These processing schemes were tested on a 2D synthetic data set with 100 shots. Each shot has a split-spread array of 100 geophones. The first shot is located at 0m with geophones between –495m and 495m. The geophone spacing is 10m, while the source spacing is 100m. There are three reflections and twenty-five diffractions in the synthetic model. Figure 3 presents the first shot gather.

Processing Schemes

Diode Filter:

(1) Each shot gather is split into positive and negative offsets.

(2) In each half gather, backscattered energy propagating toward the source is removed by dip-filtering. Forward scattered energy propagating away from the source is kept in place. The data is sorted into receiver gathers, and the procedure is repeated.

(3) This process removes "everything" but the reflection hyperbolas from the seismic section. Hence the reflection section is subtracted from the original section to generate the diffraction section. As can be seen in figure 4, all three reflection hyperbolas have weakened. However, some tails of the diffraction patterns have been removed, too, because the dip filter can not completely remove all diffraction patterns in the original section.

NMO – Dip Filter:

(1) Shot gathers are NMO corrected with the appropriate stacking velocity.

(2) After NMO correction, the reflections become flat while the diffractions hyperbolas are strongly deformed. The flat reflection events are removed by dip filtering and the remaining section is transformed back by UnNMO. The resulting gather is shown in figure 5.

DMO – NMO – Dip Filter: DMO increases the differential moveout between diffracted and reflected events (Kent et al. 1996). We applied the following processing flow:

(1) Data is sorted into common-offset gathers and is DMO corrected.

(2) NMO is applied.

(3) All flat events are removed using a dip filter.

(4) NMO is removed (fig. 6).

Singular Value Decomposition:

A 2D seismic section can be considered as a 2D matrix, which can be decomposed in eigensections with associated eigenvalues. Large eigenvalues represent stable and prominent events such as reflections, while the small eigenvalues represent unstable and less prominent features such as diffractions. If S (t, x) is our data matrix, its corresponding singular value decomposition can be written as

$$S=U.\Sigma.\ V^{T}$$

U and V are unitary matrixes containing the left and right eigenvectors of S and Σ is a diagonal matrix with the eigenvalues of S (Bihan at el, 2001).

The largest eigenvalue is set to zero, and a modified seismic section S (1) is constructed. On the modified section, reflections are weakened. However, some diffractions have been weakened, too.

The modified section is again Singular-Value decomposed, the now largest eigenvalue is removed, and transformed back to the modified section S (2). The process is repeated until more diffractions than reflections are removed. As shown in figure 7, the middle and bottom reflections have been removed. The top reflection has been weakened. However, some noise has been introduced and diffractions were affected, although they are still strong enough to identify the scatteres.

Harlan's Signal/Noise Separation Technique:

Harlan (Harlan at al, 1984) presented a signal-noise separation scheme to separate events that can be focused by a linear transformation (signal) from events that can not be focused. We assumed reflection hyperbolas as the signal and rest of the section as noise and applied the Harlan's technique. As expected we got noise and signal sections. The signal section contains the reflection hyperbolas, and the noise section has everything but the reflection hyperbolas. However, the reflections are not completely removed from the noise section. Figure 8 represents the noise section after applying Harlan's method on the original data set.

Discussion

We presented different processing flows to extract diffractions and suppress reflections in a 2D synthetic data set. Each method has its own advantages and disadvantages which allows conservative application and combination of multiple methods. The next step will be to test these schemes on a 3D synthetic dataset. Ultimately, we will apply them on 3D field data from the San Juan basin.

Acknowledgement

This work was supported by the assistant Secretary for Fossil Energy, National Energy Technology Laboratory (NETL). We would like to thank NETL project managers Thomas Mroz and Frances Toro for their support.

References

Lynn, H. B., Simon, K. M., Layman, M., Schneider, R., Bates, C. R., and Jones, M., 1995, Use of anisotropy in P-wave and S-wave data for fracture characterization in a naturally fractured gas reservoir: The Leading Edge, **14**, 887-893.

Kent, G. M., Kim, I. I., Harding, A. J., Detrick, R. S., and Orcutt, J. A., 1996, Suppression of sea-floor-scattered energy using a dip-moveout approach – application to the mid-ocean ridge environment: Geophysics, **61**, no. 3, 821-834.

Bihan, N. L., Lariani, S., and Mars, J., 2001, Seismic cube decomposition before reservoir characterisation: 71st Annual Meeting of SEG, San Antonio.

Harlan, S., Claerbout, J., and Roca, F., 1984, Signal/noise seperation and velocity estimation: Geophysics, **53**, no. 11, 1869-1880.

Daley, T. M., Nihei, K. T., Myer, L. R., Majer, E. L., Queen, J. H., Fortuna, M., Murphy, J., 2002, Numerical modeling of scattering from discrete fracture zones in a San Juan Basin gas reservoir: 72nd Annual Meeting of SEG, Salt Lake City.

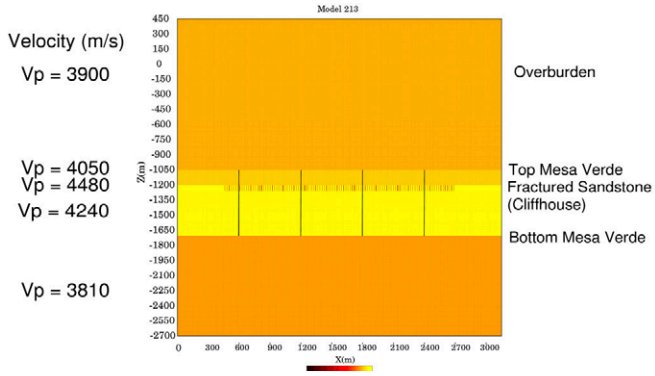

Figure 1
A model with five layers and two fractures sets. Cliffhouse sandstone is highly fractured with small aperture while, entire Bottom Mesa Verde contains small number of fractures with large aperture.

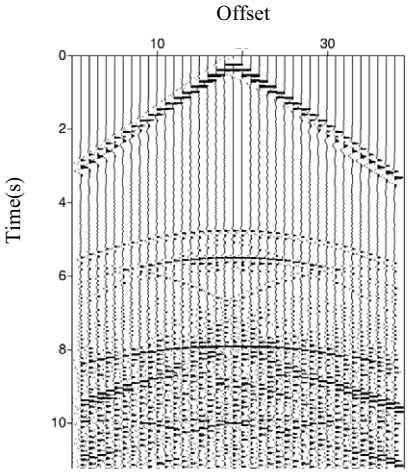

Figure 2
Seismic response of the subsurface model. Fracture responses are similar to diffractions.

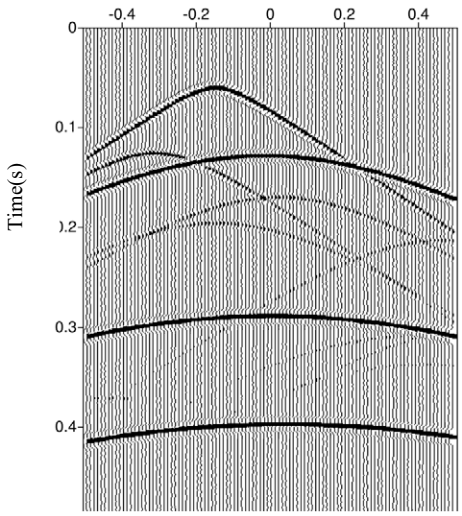

Figure 3
Unprocessed synthetic section.

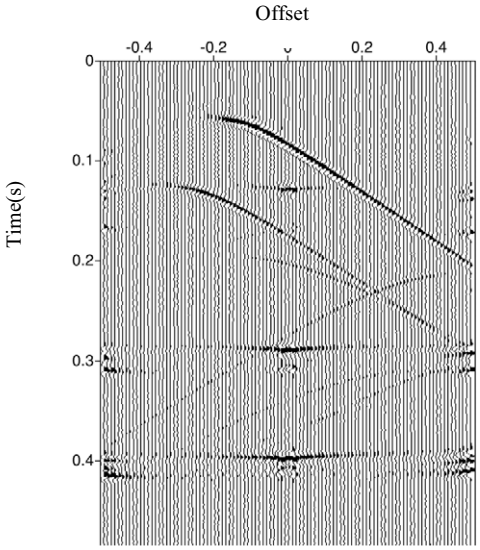

Figure 4
Processed data after diode filtering.

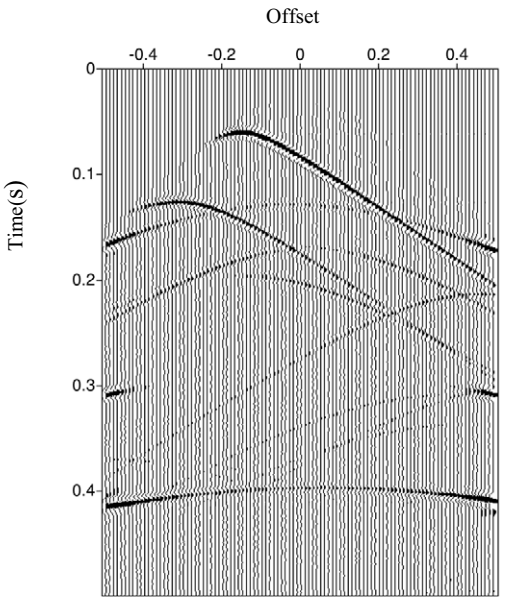

Figure 5
After applying NMO-dip filter.

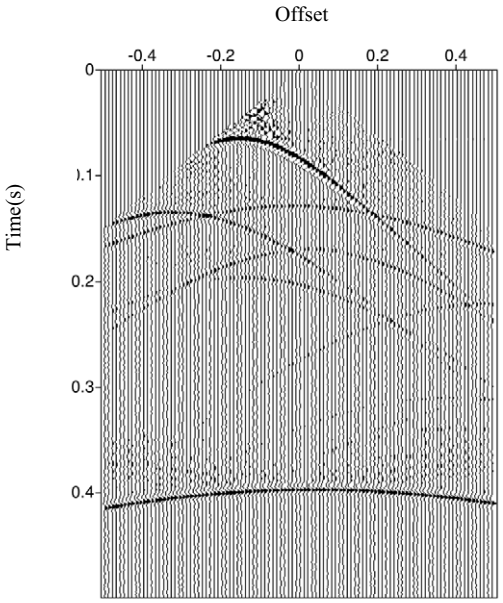

Figure 6
After applying DMO-NMO-dip filter.

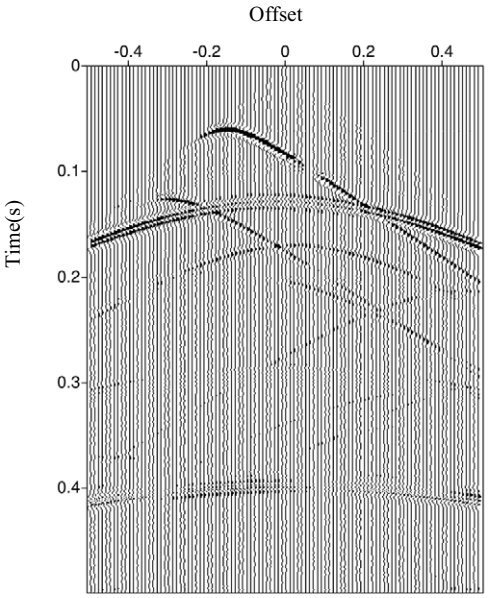

Figure 7
Processed data after applying SVD.

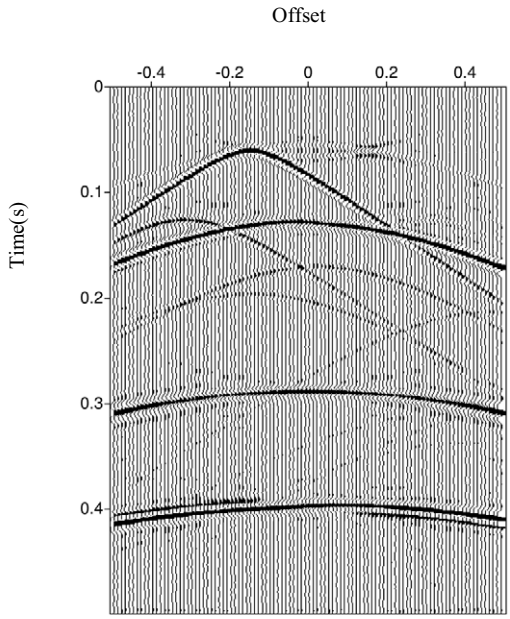

Figure 8
Noise section after applying Harlan's method.